Received: 28 October 2018 | Revised: 31 August 2019 | Accepted: 20 October 2019

DOI: 10.1002/stc.2479

RESEARCH ARTICLE

WILEY

Novel health monitoring technology for in-service diagnostics of intake separation in aircraft engines

Len Gelman[1] | **Ivan Petrunin**[2] | **Colin Parrish**[3] | **Mark Walters**[4]

[1]School of Computing and Engineering, University of Huddersfield, Huddersfield, UK

[2]School of Aerospace, Transport and Manufacturing, Cranfield University, Cranfield, Bedfordshire, UK

[3]ERTS Division, Rolls-Royce, Derby, UK

[4]Condition Monitoring Division, Hevasure Ltd., Matlock, UK

Correspondence
Ivan Petrunin, Cranfield University, Cranfield, Bedfordshire MK43 0AL, UK.
Email: i.petrunin@cranfield.ac.uk

Funding information
Innovate UK, Grant/Award Number: TP 101291

Summary

Diagnostics and elimination of airflow separation effects draw essential attention of researchers in the areas of energy generation, civil engineering, and aerospace due to unwanted and harmful interaction of separated airflow with different structures. In aviation, distortion of the intake airflows of an aircraft engine, known as intake separation, not only reduces the efficiency of the engine due to decrease in air intake but also interacts with engine structural components, for example, blades, significantly increasing their vibration. This leads to fatigue and subsequent accelerated failure of these components. Therefore, health monitoring and diagnostics of the intake separation effects using structural health monitoring (SHM) framework are of high importance for ensuring both optimal engine performance and its safe operation. In the present paper, a novel health monitoring technology based on advanced signal processing, the integrated higher order spectral technique, is applied for the first time in worldwide terms for in-service intake separation diagnostics in aircraft engine using casing vibration data.

KEYWORDS

aircraft gas turbine, diagnostics, health monitoring, higher order spectral analysis, signal processing, vibration

1 | INTRODUCTION

Investigation of flow separation effects in gas turbines is of high importance for a wide range of applications, such as energy generation, civil engineering, and aviation. Aviation is clearly one of the critical areas of application due to severity of consequences. As it is mentioned in Cohen et al,[1] the intake is a critical part of an aircraft engine installation, having a significant effect on both engine efficiency and aircraft safety.

Flow separation at the intake of aircraft engines can be caused by number of reasons, including design flaws and winds blowing across the direction of the airflow at the engine inlet or the crosswinds.[1,2] Wind is an important factor that needs to be taken in consideration. It creates excessive vibrations in tall buildings and other wind-sensitive structures, thus increasing the risks of losing their structural integrity.[3,4] In case of an aircraft engine, wind (especially the crosswind) modifies interaction of the airflow with engine inlet structures, where geometry of the intake

defines parameters of the airflow ingested by the engine and resistance to flow separation at varying operational conditions.[5]

It is known for a long time that flow separation effects in the intake due to crosswinds make a detrimental impact not only on performance of the aircraft engine but also lead to significant increase of structural vibrations, for example, blade vibrations. Therefore, timely in-service detection of the intake separation phenomena is required in order to prevent the accelerated fatigue and structural damage of aircraft engine structures, such as blades that may cause catastrophic failures of the engine and the aircraft.

Many nondestructive testing (NDT) techniques, used for damage detection in aircraft engine structures, are time-consuming and involve significant costs. The NDT inspections are normally performed off-line at a pre-defined time intervals and cannot capture the problem that can be developed after exposure of aircraft engine structures to significant excitation, for example, as a consequence of intake separation occurrence. The structural health monitoring (SHM) framework can help in addressing this problem by providing continuous information about structures being monitored from embedded sensors.[6,7]

2 | STATE OF THE ART

Vibration response of structures is an important source of information that allows for effective health monitoring of structures.[8,9] Vibration data collected from the structures in unsteady conditions, such as those due to flow separation events, will contain the forced and potentially nonlinear response of the structures (e.g., blades in case of gas turbines) to these excitations.

One of the mechanisms of inducing vibration in structures is related to their interaction with winds and, more generally, with turbulent air flows. Flow separation, as one of the reasons for creation of the turbulent airflow, usually occurs when the flow suddenly moves away from a body or a structure or returns to it. Flow separation at different conditions can lead to development of separation bubbles (if flow reattachment occurs) or to transition from laminar to turbulent flow.[10,11] In gas turbines the resulting heterogeneity of the flow may cause aerodynamic instabilities of blades or even stall.[12] It is known[13] that for certain flow configurations, airfoil emits discrete acoustic tones; that is, it vibrates. Single or multiple tones can be observed in different configurations.[14-16] It is accepted that underlying effect in all cases is hydrodynamic instability[13]; in particular, this can be due to presence of the separation bubble.[17] It has to be mentioned that the mechanism of the effect is still not fully understood,[13] but it is shown[14,16] that if multiple tones are observed, frequencies of the tones are spaced regularly.

When the excitation frequencies created by hydrodynamic instabilities are close to an eigenfrequency of a structure, such as a blade in the engine, the blade will resonate. In this case, amplitude of a blade vibration can grow significantly, leading thus to a structural damage of a blade due to fatigue. As a result of the increased vibration level, generation of additional multiple superharmonic components of the excitation frequency in a blade vibration response is expected because of its inherent structural nonlinearity.

It was shown[18] that flow separation in Lockheed C-141 Starlifter engine generates structural vibrations in blades, causing their accelerated fatigue. These structural effects are also valid for a smaller scale objects, such as industrial fans. It is confirmed experimentally[19,20] that flow distortions due to crosswinds lead to increase in levels of structural vibrations of fan blades. It was found, in particular, that both acoustic and vibration structural responses of blades due to crosswind are similar and contain multiple superharmonics of the rotation frequency as well as first eigenfrequency of the blade.

The literature review undertaken by the authors has revealed that a significant amount of publications related to investigation of flow separation events is based on the computational fluid dynamics (CFD) methods. They are able to predict a flow separation, analyze its influence on gas turbine's performance, and optimize of design for the best performance.[10,12,21-24] Therefore, numerical methods based on the CFD are powerful instruments for optimal turbine design, analysis, and prediction of the flow separation phenomena. However, due to the complexity of real turbines, variety of real conditions, and relatively high computational cost of CFD simulations, these methods are of a limited use for the in-service flow separation detection in turbines during their operation.

Present methods of experimental detection and diagnostics of flow separation events at different surfaces are rather laboratory based and rely on use of wind tunnels, instrumented with flow visualization tools: smoke or oil complemented by sensor arrays for measurement of pressure distributions, for example, Pitot and Kiel probes[1] and piezoresistive pressure sensors.[11] Instruments for measurement of the local flow velocities, such as hot wires, hot films, and laser Doppler anemometers, are also widely used.[11,12,19-22,25-28]

In contrast to the computationally complex methods of the CFD involved into numerical studies of the flow separation, experimental detection and diagnostics of the flow separation are predominantly based on simple signal processing techniques.

In works,[11,21,28] conclusions about presence of flow separation are made on the basis of visualization of flow parameters, for example, velocity and pressure profiles and contours. Other authors, in order to detect flow separation, complement flow parameter visualization by various signal processing techniques. Cross-correlation estimates between wall pressure and streamwise velocity components are analyzed by Liu et al[25]; Rudmin et al[27] consider correlation between adjacent hot film sensor signals for flow separation detection. Low order spectral estimates are frequently used to support analysis of the separated flow behavior. For example, work[25] used an autospectrum of wall pressure values for analysis of flow separation effects; study[26] implemented power spectrum and coherence of pressure measurements for analysis of a separated flow; research[27] use power spectra of hot film signals to show the difference between them before and after flow separation. Other authors[19,20] applied spectral analysis to blade vibration signals from laser scanning vibrometer to investigate effects of local flow instabilities due to crosswind on the structural vibration of an axial fan blade. Some studies implement more complex and sensitive techniques: Γ functions with entity connection graphs applied to velocity and pressure measurements[22] and autocorrelation based on the continuous wavelet, transform of pressure measurements[25] for flow separation detection, diagnostics, and analysis.

Experimental studies in the above publications present measurement methodologies, test rigs, corresponding signal processing techniques, and results with great amount of details for aerodynamic research and design purposes. Unfortunately, their application to in-service flow separation diagnostics in the mass production gas turbines, such as aircraft engines, is not possible due to intrusive nature of measurements, complexity of both post-processing, and analysis of results. Also, none of the publications found by authors consider flow separation diagnostics using nonintrusive measurements, such as structural vibration signals (from casing vibration sensors), which are already present in many aircraft engines.

Vibration signals acquired by sensors on engine casing contain large number of components related to flow separation effects, other phenomena (not related to flow separation), and a wideband noise. Such a complex combination sets high requirements to signal processing techniques, which may be used for extraction of information about flow separation from the structural vibration signal. Therefore, considering detection of the flow separation effects using vibrations of an aircraft engine, it can be concluded that signal processing techniques mentioned above are not optimal for flow separation diagnostics in terms of their sensitivity and immunity to a wideband noise.

Here, the higher order spectral (HOS) techniques may deliver better results. These techniques are well understood and interpreted[29]; they were successfully applied for a wide variety of problems, including detection of nonlinearities in structures,[7,30] machine fault diagnosis,[31] and fatigue testing.[32] The HOS techniques are also known to have superior sensitivity to weak signals on the background of a strong noise[33] in comparison with low order spectra, such as the power spectral density.

At the present time, there are no published works related either to use of the HOS technologies for flow separation diagnostics or design of diagnostic features suitable for such tasks. Explanation to this fact, in our opinion, can be given by complex nature of the interaction between intake flow and engine's components, difficulties with analysis of HOS technologies for such a complex signals and problems with adaptation of HOS techniques to nonstationary intake separation phenomena, which generally require both nonlinear SHM approach and nonlinear techniques, such as those discussed in Ciampa et al.[7]

As a consequence, even known promising higher order techniques cannot be directly applied for intake separation detection due to complex nature of intake separation event and, therefore, complex nature of vibration signals related to this event.

So, the problem considered in this paper concerns development of a novel health monitoring technology for intake separation diagnostics that will take into account complex nature of structural vibration related to the intake separation event.

Therefore, objectives of the present paper are as follows:

1. To develop and investigate for the first time in worldwide terms a novel health monitoring technology for intake separation diagnostics based on signal processing of structural vibrations from an aircraft engine.
2. To perform novel optimization of parameters of the developed technology.
3. To obtain novel experimental results related to efficiency of the developed technology.

3 | THEORETICAL BACKGROUND

In the previous section, we discussed that the novel signal processing techniques, the higher order spectra (HOS) technologies, may help in identification of flow separation at the aircraft engine's intake based on the engine vibration data. Due to high sensitivity to presence of phase coupling between spectral components,[29] which are produced as a result of intake separation and consequent nonlinear effects due to high amplitude of the structural vibrations, the HOS technologies may provide information that will allow diagnostics of flow separation effects. There are two important problems on the way of development of the HOS techniques for in-service diagnostics of intake separation.

The first problem is how to develop novel signal processing based on the HOS technologies, generally suitable for stationary data only,[29] to essentially nonstationary signals.

The second problem is related to limited knowledge about amount of available diagnostic information: number of components created or affected by presence of intake separation, uncertainties about their localization in frequency domain, and amplitudes.

In order to solve both problems, the novel health monitoring technology developed here for intake separation diagnostics is based on the novel signal processing: the nonstationary integral higher order measure of vibration signal nonlinearity due to intake separation event. To enable the proposed integral measure to reflect the time variation of summed components, the short time HOS technique[34] is further developed here for the technology. In order to address the above-mentioned problems, the nonstationary HOS technique is developed for the vibration data represented by a number of overlapping records, covering the whole duration of the analyzed signal

$$B_n(f_k,f_l)=\frac{\sum_i X_i(f_k)X_i(f_l)X_i^*(f_k+f_l)}{\sqrt{\sum_i |X_i(f_k)X_i(f_l)|^2\sum_i |X_i(f_k+f_l)|^2}}, \tag{1}$$

where B_n is the computed amplitude value of normalized short time higher order spectrum for the nth record at frequency coordinates (f_k, f_l), $X_i(f_k)$, $X_i(f_l)$, and $X_i(f_k+f_l)$ are the Fourier transforms of the data segment i for the spectral components k, l, and $k+l$ with frequencies f_k, f_l, and f_k+f_l; $i = 1,...,M$, M is the number of the data segments forming the nth data record, * is a symbol of the complex conjugate.

The computed value of B_n contains multiple components at various frequency coordinates. Some of these components are related to appearance of the intake separation and change their amplitudes as intake separation occurs. Other components will not be changing due to intake separation and describe a baseline of the engine operation.

The novel health monitoring technology proposed here for intake separation diagnostics is based on summing the squared magnitudes of the short time higher order spectrum (Equation 1). Only those values that exceed the selected threshold T are selected for the technology. A background level of the short time higher order spectrum is considered as an interference for the proposed technology and is removed from the computed feature. This is reflected in the expression of the diagnostic feature, shown below:

$$S_n(T)=\sqrt{\sum_{i=1}^{N}\left(\sum_{\substack{f_{ki\min}<f_{ki}\le f_{ki\max}\\ f_{li\min}<f_{li}\le f_{li\max}}}\left\{|B_n(f_{ki},f_{li})|^2\big|_{|B_n(f_{ki},f_{li})|\ge T}-\frac{1}{M}\sum_{\substack{f_{ki\min}<f_{ki}\le f_{ki\max}\\ f_{li\min}<f_{li}\le f_{li\max}}}|B_n(f_{ki},f_{li})|^2\big|_{|B_n(f_{ki},f_{li})|<T}\right\}\right)} \tag{2}$$

where $f_{ki\min}$, $f_{ki\max}$ and $f_{li\min}$, $f_{li\max}$ are the frequency coordinates of the ith local rectangular area for the background value calculation; $i = 1,...,N$, N is the number of local rectangular areas in the analyzed HOS; M is the number of components of the short time HOS below the threshold T.

The rectangular area of the HOS, utilized for calculation in Equation (2), is illustrated in Figure 1. Let us assume threshold $T = 0.3$ in this example. We can see in Figure 1 that there is only one high magnitude component, exceeding the threshold, in the analyzed rectangular area and the magnitude value of this component is used for summation in Equation (2). All other HOS values in the considered rectangular area are below threshold and are used for estimation of the background noise, which is removed from each high magnitude component.

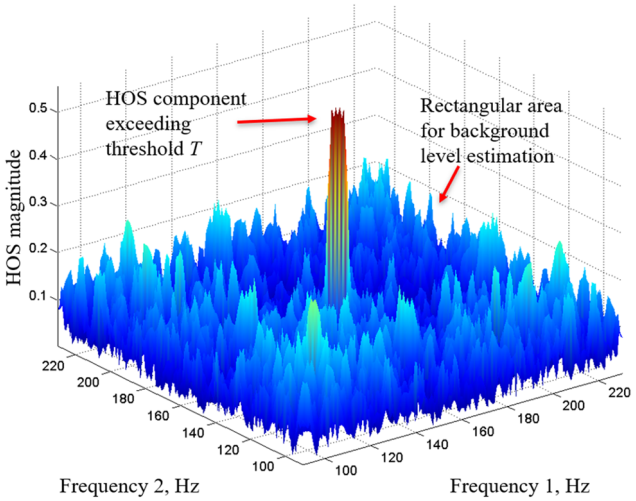

FIGURE 1 Background noise levels in the rectangular local area of the HOS and one high magnitude HOS component

In this scheme, threshold T helps to sum components with essential amplitudes only and, therefore, minimizes influence of the background noise. In practice, values of the threshold T could be chosen in the range from 0.2 to 0.9.

4 | EXPERIMENTAL DATA DESCRIPTION

Experimental data sets represent two recordings of an aircraft engine run-up in a crosswind condition. Run-up parameters for these signals represent typical conditions of the engine start up; therefore, it is anticipated that the results of the analysis performed below could be applicable in many practical situations.

Signals representing structural vibration of the engine were acquired from two sensor types: a casing accelerometer and a strain gauge installed on one of the fan blades. Strain gauges were installed on two different blades for these two run-ups.

The data from the casing accelerometer demonstrate a mixture of the multiple components both wideband and narrowband from various sources. Identification of weak signals in this mixture often becomes complex. Therefore, in order to identify time limits of the intake separation event and to provide a time reference for efficiency estimation of the proposed health monitoring technology, the data from the strain gauges are used. The time identification is performed according to analysis of the short time Fourier transform (STFT) of the strain gauge data. Once time limits for intake separation event are identified, the signal processing for event diagnostics is performed using the accelerometer data.

The STFT of the strain gauge data normalized with respect to its maximum value for the first data set is shown in Figure 2. It can be seen that in the time interval from 24 to 29 s, there is a number of clearly visible spectral components

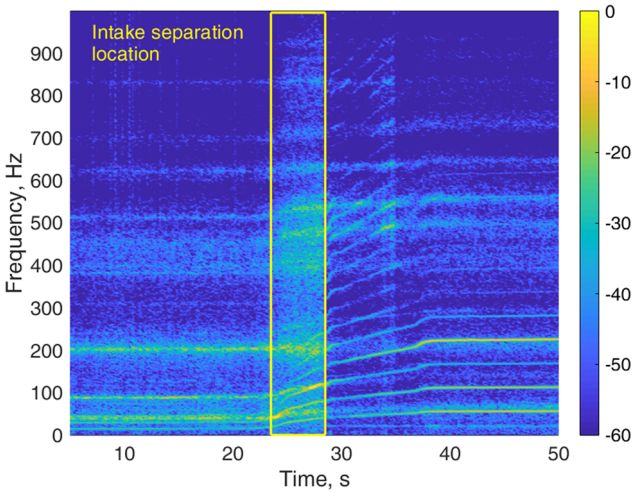

FIGURE 2 The normalized short time Fourier transform of the strain gauge data with Z-axis represented by color and expressed in dB scale for first engine run-up

in the frequency range of up to 900 Hz. The components are both narrowband and wideband, due to the intake separation event.

The STFT of the casing accelerometer (Figure 3) in the chosen time interval shows less components than the STFT of the strain gauge data with exception for a frequency range of up to 100 Hz. Components from vibration data are also less intensive compared with components from the strain gauge data. Strong components can be seen in the accelerometer data STFT a few seconds prior to the beginning of the intake separation event (identified from the strain gauge data). These components may represent Lresponses from other blades, also affected by the intake separation.

The time and the frequency range for the signal processing are set according to observations of the strain gauge data. Therefore, it is accepted here that vibration data within 24–29 s range from the beginning of the file contain signatures of the intake separation event. In order to form a reliable baseline of normal engine vibrations, the data fragments located outside of the identified time limits of the event are selected. Following this strategy, the data before 20th second of the record and after 40th second are identified as suitable for the baseline. According to visual observations of both STFT results (Figures 2 and 3), there are no signatures of the intake separation events in the chosen intervals.

Similar procedure was applied to the second data set. STFT plots of the strain gauge and accelerometer data were calculated using same parameters as for the first data set and are shown in Figures 4 and 5, respectively.

Both STFT plots demonstrate features similar to those from the first run-up data. According to the STFT of strain gauge data, the intake separation event is located within the interval 20–24 s of the data record; this information will be used later, during the result analysis.

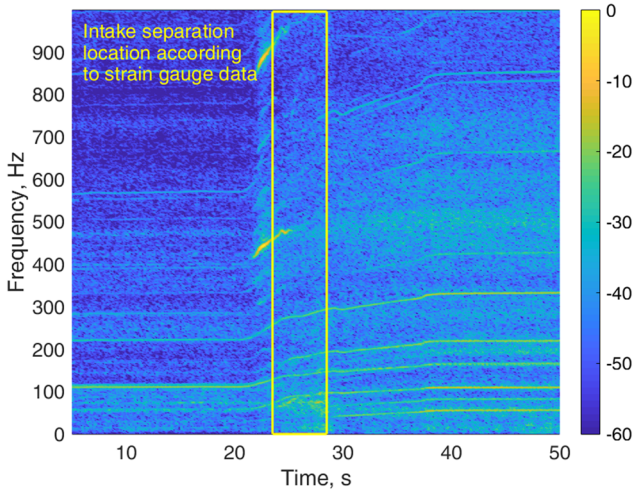

FIGURE 3 The normalized short time Fourier transform of the accelerometer data with *Z*-axis expressed in dB scale for first engine run-up

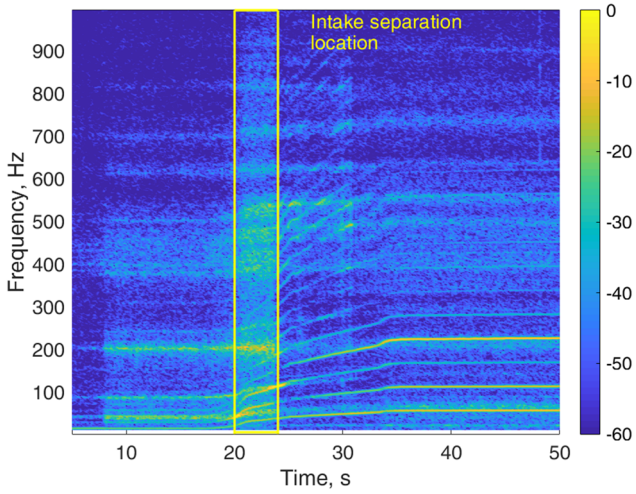

FIGURE 4 The normalized short time Fourier transform of the strain gauge data with *Z*-axis represented by color and expressed in dB scale for second engine run-up

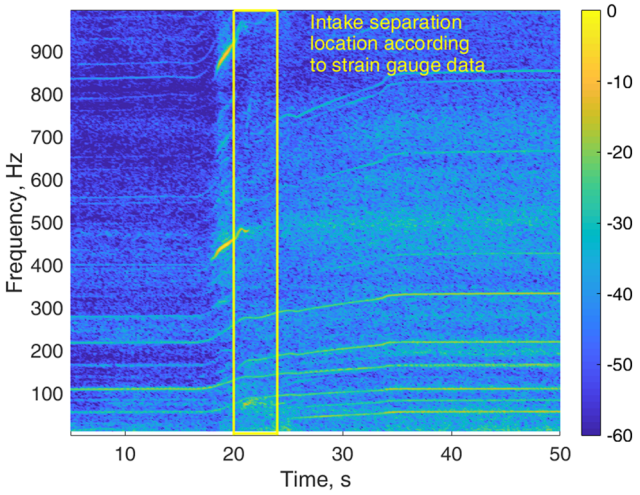

FIGURE 5 The normalized short time Fourier transform of the accelerometer data with *Z*-axis expressed in dB scale for second engine run-up

5 | ANALYSIS OF RESULTS AND TECHNOLOGY PARAMETER OPTIMIZATION

The diagnostic feature, defined by Equation (2), was calculated for both engine run-ups using the accelerometer data. In order to evaluate the effectiveness of the diagnostic feature for diagnostics of the intake separation, the Fisher criterion[35] was proposed:

$$F = (\mu_2 - \mu_1)^2 / (\sigma_1^2 + \sigma_2^2), \tag{3}$$

where μ_1, μ_2, σ_1^2, σ_2^2 are the mean values and the variances for two groups of the diagnostic features being analyzed.

The Fisher criterion in Equation (3) characterizes numerically separation between the diagnostic features obtained for a time period when intake separation is observed and for periods where there are no intake separation signatures found.

Optimization of the main diagnostics parameters was performed for the first run-up data and was based on maximization of the proposed efficiency criterion (Equation 3). Parameters optimized are those describing the proposed diagnostic feature (Equation 1): record size (starting from 3 to 10 s with 1 s step) and segment size (from 0.3 s to 1 s with 0.1 s step). The overlap between the segments and the time step between the consequent records were constant and equal to 65% and 1 s, respectively. The Hamming weighting window was applied to the segment data in both cases. As the amount of the experimental data is limited, it was decided to increase it by multiple additions of a small amount of a random noise, unique for each addition. Thus, for each parameter combination, 20 repeat signal processing estimations were performed with addition of the Gaussian noise to the vibration data, using the signal to noise ratio of 30 dB. Separate optimization for threshold T in expression of the diagnostic feature (Equation 2) was performed in the interval from 0.2 to 0.9 with the step of 0.1.

In terms of the Fisher criterion (Equation 3), characterizing the separation between the diagnostic features inside and outside of the intake separation area, the best results were obtained using the external window size of 4 s and the segment size of 0.5 s.

Values of the short time higher order spectrum (Equation 1) within the range 0–1000 Hz for both frequency axes, representing the first quadrant of the bi-frequency plane, are shown in Figures 6–8. Figure 6 is calculated for the time range before the beginning of intake separation (from 16 to 20 s of the accelerometer data), Figure 7 is for the intake separation time range (from 24 to 28 s of the accelerometer data), and Figure 8 is for the time range after the intake separation area (from 40 to 44 s of the accelerometer data).

As one can see from Figures 6–8, the short time higher order spectrum for the data representing the intake separation visually contains more components with magnitudes in the range 0.2–0.4 than the short time higher order spectrum for the data without the intake separation. The histograms of the raw HOS values for the results shown in Figures 6–8 are presented in Figure 9. It can be seen that histograms of HOS values before and after intake separation demonstrate a lot

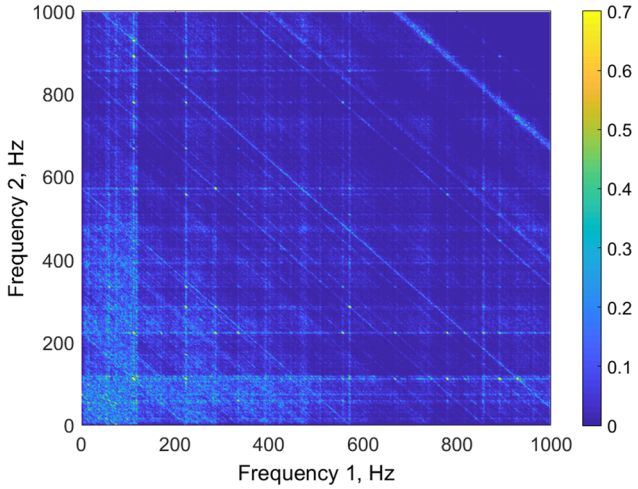

FIGURE 6 Magnitude values of the short time higher order spectrum before the beginning of the intake separation event for the first run-up data

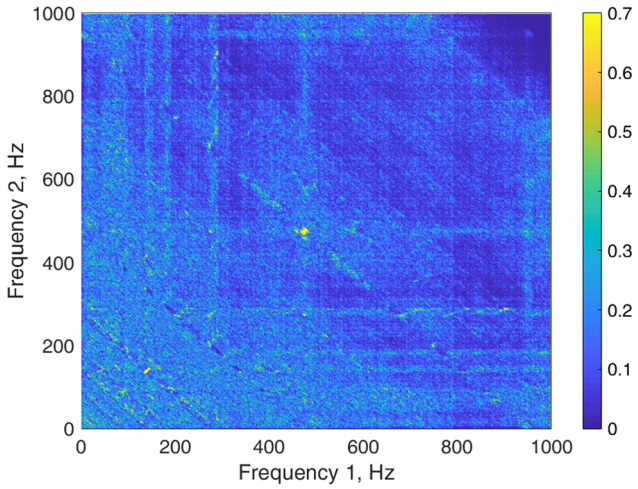

FIGURE 7 Magnitude values of the short time higher order spectrum during the intake separation event for the first run-up data

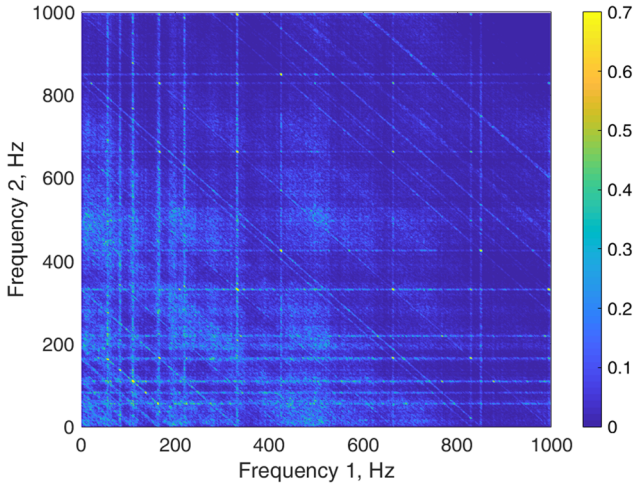

FIGURE 8 Magnitude values of the short time higher order spectrum after the end of the intake separation event for the first run-up data

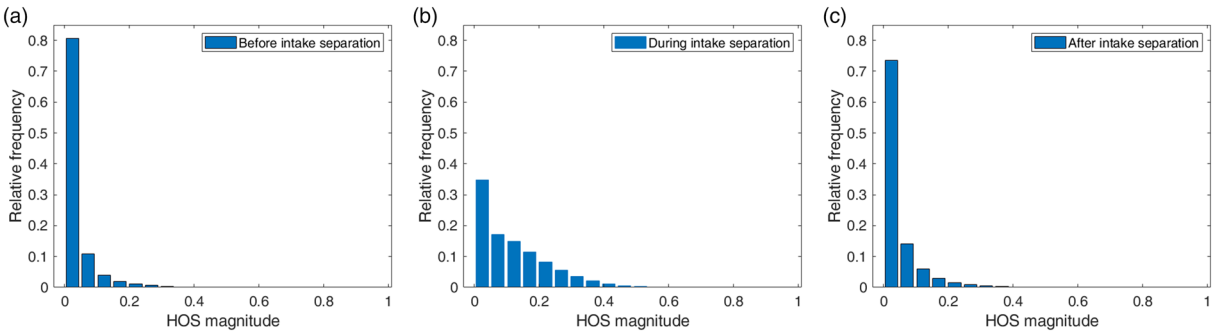

FIGURE 9 Histogram of the raw HOS values for the first run-up data before the intake separation (left), during the intake separation (center), and after the intake separation (right)

of similarity in behavior; therefore, we can combine them for comparison with the histogram of the HOS during the intake separation. The combined histograms for raw magnitude values of the HOS for cases when intake separation is present and is not present are shown in Figure 10.

One can see from Figure 10 that the histograms are essentially overlapped that makes detection of the intake separation using raw HOS values complicated. One can observe from Figure 10 that use of simple thresholding of raw HOS will not provide good diagnostic results.

The effectiveness of the health monitoring technology proposed here for intake separation diagnostics depends on threshold T chosen for summation in Equation (2). Using the data for the first run-up, this dependency was evaluated and shown in Figure 11.

It can be seen that a good separation between the cases, in which intake separation is or is not present, could be achieved in the range of thresholds 0.2–0.5 with the maximum at the threshold value of 0.4. The values of the Fisher criterion (Equation 3) are low after the value of the threshold of 0.6. The histograms of the diagnostic features (Equation 2) for the areas without and with the intake separation obtained for optimal threshold value for the first run-up data are shown in Figure 12.

For in-service diagnostics of the intake separation, a comparison with the detection threshold T_D can be used. It can be seen from the histograms in Figure 12 that there is a full separation between the features, characterizing the normal operation of the aircraft engine, and operation of the aircraft engine with presence of the intake separation. The error-free diagnostics can be potentially achieved using the detection threshold T_D, set in the range of values of the diagnostic feature (Equation 2) from 13 to 20.

The signal processing of the second data set was done using parameters, obtained during the optimization procedure based on the first run-up data. This approach reproduces worst case scenario of real-life conditions when it is not possible to fine tune parameters for every data to be processed.

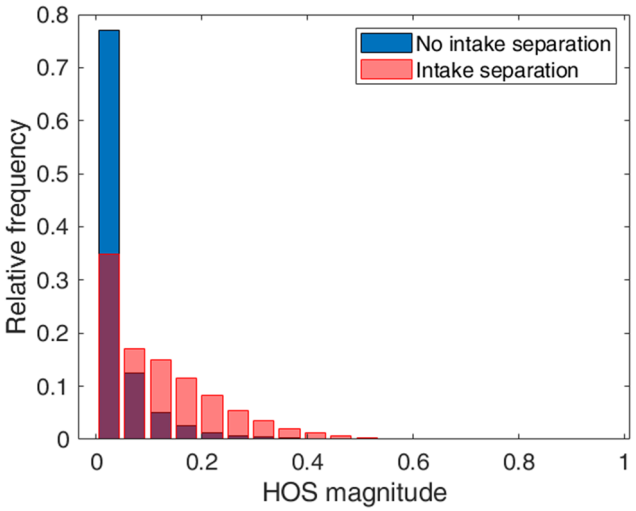

FIGURE 10 Histograms of the raw HOS values for the first run-up data

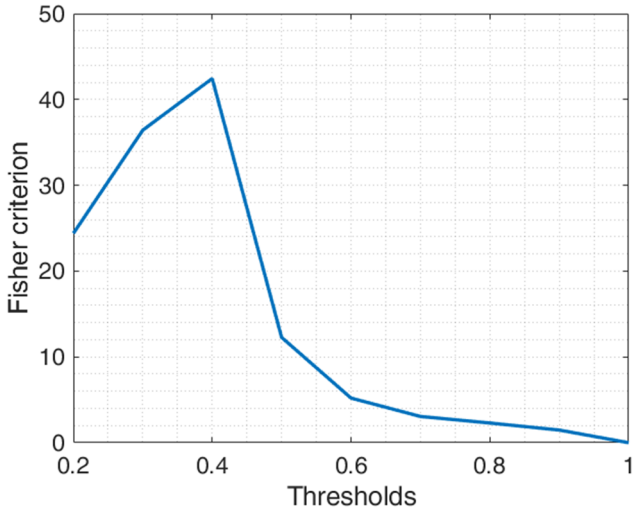

FIGURE 11 Dependency of the Fisher criterion value on summation threshold

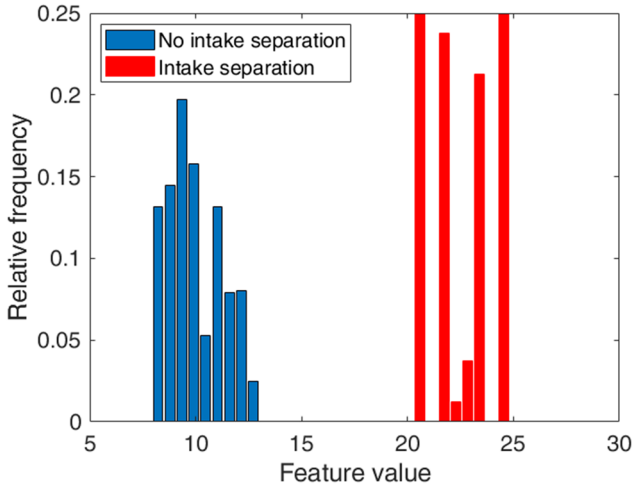

FIGURE 12 Histograms of the diagnostic features for the first run-up data

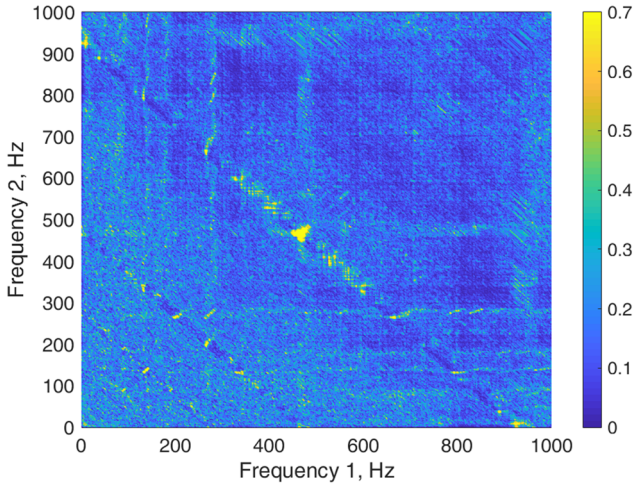

FIGURE 13 Magnitude values of the short time higher order spectrum during the intake separation event for the second run-up data

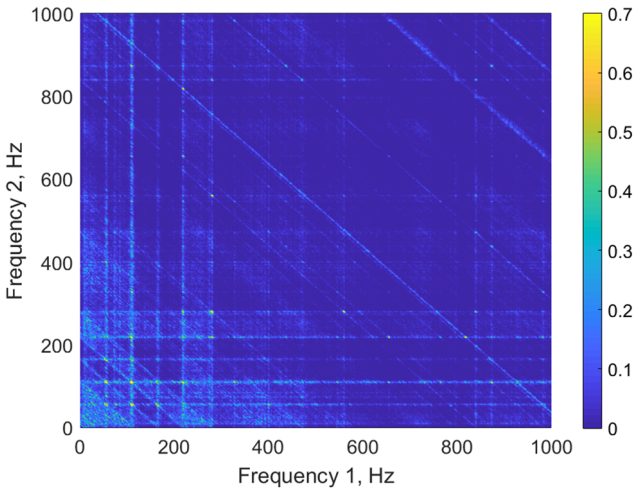

FIGURE 14 Magnitude values of the short time higher order spectrum before the beginning of the intake separation event for the second run-up data

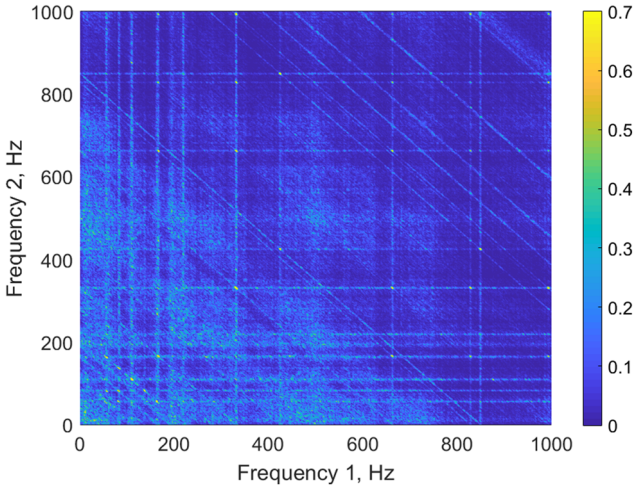

FIGURE 15 Magnitude values of the short time higher order spectrum after the end of the intake separation event for the second run-up data

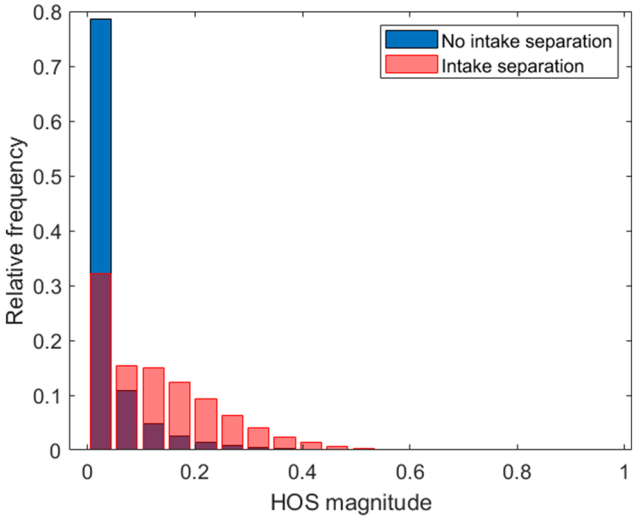

FIGURE 16 Histograms of the raw HOS values for the second run-up data

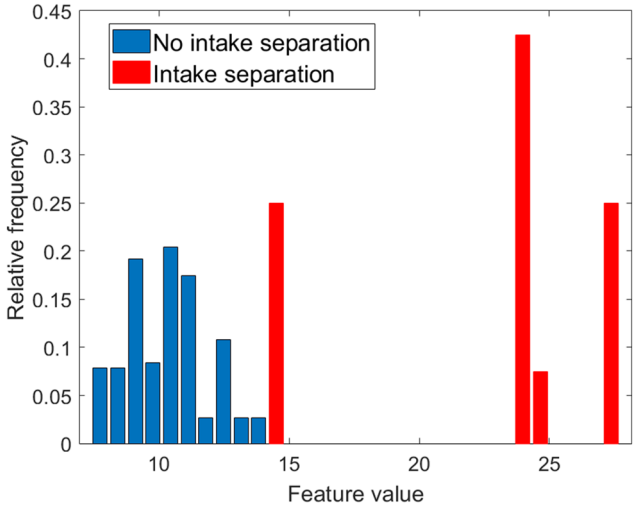

FIGURE 17 Histograms of the diagnostic features for the second run-up data

A deeper insight into behavior of the diagnostic features for second run-up data can be given by considering the short time higher order spectrum values within the interval of identified intake separation phenomenon (Figure 13) and outside of it (Figures 14 and 15). One can see that the short time higher order spectrum obtained using the data from time interval 20–24 s (Figure 13), which represents the intake separation event, has significant number of components with amplitudes 0.4–0.5. There are also many components with larger amplitudes.

At the same time, both the short time higher order spectra for data before (Figure 14) and after (Figure 15) intake separation are significantly quieter.

The areas representing the engine condition before, during and after the intake separation were designated according to Figure 4. Taking an advantage of that information, histograms of raw HOS values (Figure 16) and the diagnostic features (Figure 17) were obtained using the same signal processing methodology as for the first run-up data. The same parameters, obtained as a result of optimization performed for the first run-up data, were used here: record size of 4 s and segment size of 0.5 s with overlap between segments fixed at 65% level.

One can see from Figure 16 that the histograms related to the raw HOS values are essentially overlapped for the cases of with and without intake separation. One can observe from Figure 16 that use of simple thresholding of raw HOS data will not provide good diagnostic results. So, diagnostics of the intake separation, using the raw HOS values, is noneffective. From the histograms shown in Figure 17, one can see that the health monitoring technology, proposed in this paper for intake separation diagnostics, performs well and provides a full separation between diagnostic features representing intake separation event and baseline data (with optimal selection of the detection threshold T_D).

Optimal detection threshold T_D for this case is 14.2; it falls into the interval of optimal detection thresholds, obtained for the first data set: 13 to 20. In case of nonoptimal selection of parameters for the proposed technology, its performance will somewhat degrade, but overall performance remains fairly high as it can be seen from the results with nonoptimal parameter selection in Figure 17.

6 | CONCLUSIONS

The novel generic health monitoring technology for in-service diagnostics of the intake separation in aircraft engines is proposed and experimentally validated in this paper for the first time in worldwide terms. The technology is based on the novel integrated diagnostic feature, extracted from structural vibration data of an aircraft engine. The research, described in this paper, is promising and leading in the research area, related to nonlinearity diagnostics in aircraft engines.

As a result of the extensive literature review, covering the physical background of a flow separation phenomenon, its influence on reliability of an aircraft engine and the approaches for flow separation detection, a novel signal processing technique was identified that is suitable for in-service health monitoring and diagnostics of the intake separation based on the engine vibration signal. Novel integrated diagnostic feature was designed using the identified signal processing technique.

Novel experimental investigation of this diagnostic feature, applied to an aircraft engine vibration data with and without intake separation, has shown a distinctive difference between these cases: Value of the proposed integrated feature increases significantly when intake separation present. Following this finding, the novel health monitoring technology, based on the integral measure, was developed.

Optimization of the signal processing parameters of the proposed technology, maximizing the separation between diagnostic features, has been performed. As a result, full separation between the diagnostic features for the data with intake separation event and without event was achieved for two real-life examples of the aircraft engine run-up data. Full separation between the diagnostic features demonstrates a potential of the proposed health monitoring technology for error-free health monitoring and diagnostics of the intake separation with corresponding reduction of a structural damage risk and extension of the service life of engine's structural components.

The proposed technology presents a fundamental new concept; it will make a major influence on health monitoring and diagnostics of nonlinear effects in aircraft engines and other types of rotating machinery and also can be effectively employed for other nonlinear structural health monitoring tasks.

ACKNOWLEDGEMENT

The authors thankfully acknowledge the financial support of this work by Innovate UK (Grant TP 101291).

ORCID

Ivan Petrunin https://orcid.org/0000-0002-8705-5308

REFERENCES

1. Cohen H, Rogers GFC, Saravanamuttoo HIH. *Gas Turbine Theory*. 4th ed. Harlow: Longman; 1996.
2. Shedon J, Goldsmith EL. *Intake Aerodynamics*. 2nd ed. Oxford: Blackwell Science; 1999.
3. Zhi L, Fang M, Li QS. Estimation of wind loads on a tall building by an inverse method. *Struct Control Health Monit*. 2017;24(4):1-21, e1908. https://doi.org/10.1002/stc.1908
4. Simiu E, Yeo D. *Wind Effects on Structures: Modern Structural Design for Wind*. 4th ed. Hoboken, NJ: Wiley-Blackwell; 2019.
5. Sóbester A. Tradeoffs in jet inlet design: a historical perspective. *J Aircr*. 2007;44(3):705-717. https://doi.org/10.2514/1.26830
6. Pieczonka L, Zietek L, Klepka A, Staszewski WJ, Aymerich F, Uhl T. Damage imaging in composites using nonlinear vibro-acoustic wave modulations. *Struct Control Health Monit*. 2018;25(2):1-13, e2063. https://doi.org/10.1002/stc.2063
7. Ciampa F, Pickering SG, Scarselli G, Meo M. Nonlinear imaging of damage in composite structures using sparse ultrasonic sensor arrays. *Struct Control Health Monit*. 2017;24(5):1-13, e1911. https://doi.org/10.1002/stc.1911
8. Oliveira G, Magalhães F, Cunha Á, Caetano E. Vibration-based damage detection in a wind turbine using 1 year of data. *Struct Control Health Monit*. 2018;25(11):1-22, e2238. https://doi.org/10.1002/stc.2238
9. Habtour E, Cole DP, Riddick JC, et al. Detection of fatigue damage precursor using a nonlinear vibration approach. *Struct Control Health Monit*. 2016;23(12):1442-1463. https://doi.org/10.1002/stc.1844
10. Kenwright DN. Automatic detection of open and closed separation and attachment lines. In: *Proceedings Visualization'98 (Cat. No.98CB36276)*. Vol 98. IEEE; 1998:151-158. https://doi.org/10.1109/VISUAL.1998.745297
11. Schreyer A-M, Würz W, Krämer E, Talamelli A, Alfredsson H. Experimental flow studies on separation and reattachment in the vicinity of sharp, wedge shaped leading edges at low Reynolds numbers. *Notes Numer Fluid Mech Multidiscip Des*. 2010;112:273-280. https://doi.org/10.1007/978-3-642-14243-7_34
12. Colin Y, Aupoix B, Boussuge JF, Chanez P. Prediction of crosswind inlet flows: some numerical and modelling challenges. In: *Proceedings of the 18th ISABE Conference*. ; 2007:1-13.
13. Jones LE, Sandberg RD. Numerical analysis of tonal airfoil self-noise and acoustic feedback-loops. *J Sound Vib*. 2011;330(25):6137-6152. https://doi.org/10.1016/j.jsv.2011.07.009
14. Arbey H, Bataille J. Noise generated by airfoil profiles placed in a uniform laminar flow. *J Fluid Mech*. 1983;134:33-47. https://doi.org/10.1017/S0022112083003201
15. Nash EC, Lowson MV, McAlpine A. Boundary-layer instability noise on aerofoils. *J Fluid Mech*. 1999;382:27-61. https://doi.org/10.1017/S002211209800367X
16. Desquesnes G, Terracol M, Sagaut P. Numerical investigation of the tone noise mechanism over laminar airfoils. *J Fluid Mech*. 2007;591:155-182. https://doi.org/10.1017/S0022112007007896

17. Lowson M, Fiddes S, Nash E. Laminar boundary layer aero-acoustic instabilities. In: *32nd Aerospace Sciences Meeting and Exhibit*. Reston, Virigina: American Institute of Aeronautics and Astronautics; 1994. https://doi.org/10.2514/6.1994-358
18. Cleveland FA, Gilson RD. Development highlights of the c-141 starlifter. *J Aircr*. 1965;2(4):278-287. https://doi.org/10.2514/3.43653
19. Heinemann T, Münsterjohann S, Zenger F, Becker S. Cross wind influence on noise emission and computed vibrational noise of an axial fan. In: *ASME Turbo Expo 2015: Turbine Technical Conference and Exposition, Volume 1: Aircraft Engine; Fans and Blowers; Marine*. ASME; 2015:V001T09A004. https://doi.org/10.1115/GT2015-42444
20. Heinemann T, Becker S. Cross wind influence on the flow field and blade vibration of an axial fan. In: *17th International Symposium on Applications of Laser Techniques to Fluid Mechanics*. ; 2014:7-10. https://doi.org/10.1115/IMECE2011-63157
21. Biesinger T, Kappies W, Matyschok B, Stoffel B. Losses in air intake components of industrial gas turbines. In: *6th European Conference on Turbomachinery Fluid Dynamic and Thermodynamics*. ; 2005:521-531. http://tubiblio.ulb.tu-darmstadt.de/31552/.
22. Snider S, Morse D, Chen G, Apte SSV, Liburdy JJA, Zhang E. Detection and analysis of separated flow induced vortical structures. In: *46th AIAA Aerospace Sciences Meeting and Exhibit*. ; 2008:1-14. https://doi.org/10.2514/6.2008-361
23. Soemarwoto BI, Boelens OJ, Kanakis T. Aerodynamic design of gas turbine engine intake duct. *Aircr Eng Aerosp Technol*. 2016;88(5):605-612. https://doi.org/10.1108/AEAT-02-2015-0063
24. Lobo B, Zori L, Galpin P, Holmes W. Efficient modeling strategy of an axial compressor fan-stage under inlet distortion. In: *ASME Turbo Expo 2016: Turbomachinery Technical Conference and Exposition, Volume 2A: Turbomachinery*. ASME; 2016:V02AT37A039. https://doi.org/10.1115/GT2016-57467
25. Liu YZ, Ke F, Sung HJ. Unsteady separated and reattaching turbulent flow over a two-dimensional square rib. *J Fluids Struct*. 2008;24(3):366-381. https://doi.org/10.1016/j.jfluidstructs.2007.08.009
26. Siauw WL, Bonnet J, Tensi J, Cattafesta L. Physics of separated flow over a NACA 0015 airfoil and detection of flow separation. In: *47th AIAA Aerospace Sciences Meeting Including The New Horizons Forum and Aerospace Exposition*. Reston, Virigina: American Institute of Aeronautics and Astronautics; 2009. https://doi.org/10.2514/6.2009-144
27. Rudmin D, Benaissa A, Poirel D. Detection of laminar flow separation and transition on a NACA-0012 airfoil using surface hot-films. *J Fluids Eng*. 2013;135(10):101104-1-101104-6. https://doi.org/10.1115/1.4024807
28. Mahu R, Popescu F. Experimental Approach of the Turbulent Separated Flow. *Termotehnica*. 2013;1:91-94.
29. Nikias CL, Petropulu AP. *Higher-order spectra analysis: a nonlinear signal processing framework*. Englewood Cliffs, N.J.: PTR Prentice Hall; 1993.
30. Nichols JM, Olson CC. Optimal bispectral detection of weak, quadratic nonlinearities in structural systems. *J Sound Vib*. 2010;329(8):1165-1176. https://doi.org/10.1016/j.jsv.2009.10.032
31. Jiang L, Liu Y, Li X, Tang S. Using bispectral distribution as a feature for rotating machinery fault diagnosis. *Meas J Int Meas Confed*. 2011;44(7):1284-1292. https://doi.org/10.1016/j.measurement.2011.03.024
32. Jasinski M, Radkowski S. Use of the higher spectra in the low-amplitude fatigue testing. *Mech Syst Signal Process*. 2011;25(2):704-716. https://doi.org/10.1016/J.YMSSP.2010.06.001
33. Hinich MJ. Detecting a transient signal by bispectral analysis. *IEEE Trans Acoust*. 1990;38(7):1277-1283. https://doi.org/10.1109/29.57556
34. Gelman L, Petrunin I. Time-frequency higher-order spectra with adjustment to the instantaneous frequency variation. *Int J Adapt Control Signal Process*. 2010;24(3):178-187. https://doi.org/10.1002/acs.1096
35. Young TY, Fu KS. *Handbook of Pattern Recognition and Image Processing*. Academic Press; 1986.

How to cite this article: Gelman L, Petrunin I, Parrish C, Walters M. Novel health monitoring technology for in-service diagnostics of intake separation in aircraft engines. *Struct Control Health Monit*. 2020;27:e2479. https://doi.org/10.1002/stc.2479